



**HAL**  
open science

## An Uplink Analytical Model for Two-Tiered 3G Femtocell Networks

Zhenning Shi, He Wang, Ming Zhao, Mark C. Reed

► **To cite this version:**

Zhenning Shi, He Wang, Ming Zhao, Mark C. Reed. An Uplink Analytical Model for Two-Tiered 3G Femtocell Networks. WiOpt'10: Modeling and Optimization in Mobile, Ad Hoc, and Wireless Networks, May 2010, Avignon, France. pp.608-613. inria-00503107

**HAL Id: inria-00503107**

**<https://inria.hal.science/inria-00503107>**

Submitted on 16 Jul 2010

**HAL** is a multi-disciplinary open access archive for the deposit and dissemination of scientific research documents, whether they are published or not. The documents may come from teaching and research institutions in France or abroad, or from public or private research centers.

L'archive ouverte pluridisciplinaire **HAL**, est destinée au dépôt et à la diffusion de documents scientifiques de niveau recherche, publiés ou non, émanant des établissements d'enseignement et de recherche français ou étrangers, des laboratoires publics ou privés.

# An Uplink Analytical Model for Two-Tiered 3G Femtocell Networks

Zhenning Shi<sup>‡</sup>, He Wang<sup>\*†</sup>, Ming Zhao<sup>†\*</sup>, and Mark C. Reed<sup>†\*</sup>

<sup>\*</sup>The Australian National University

<sup>†</sup>NICTA, Canberra Research Laboratory

<sup>‡</sup>Alcatel Lucent-Shanghai Bell

Email: Jackson.Wang@nicta.com.au

**Abstract**—This paper proposes an analytical model to investigate the impact of interference on the uplink capacity and coverage in a WCDMA network where macrocell and femtocells co-exist. Geometric modeling for the hierarchical system is used where the randomly deployed femtocells are within the planned macrocells' topology. The interference effects among femtocells and between femtocells and macrocells are studied analytically to quantify the system capacity and coverage based on the practical target signal-to-interference ratio (SIR). Interference level splitting results show that the macrocell attached User Equipment (UE) to Home Node B (HNB) interference has severe impact on the capacity and coverage of femtocell network. Further study suggests that advanced receivers which cancel interference at the femtocell could minimize the effect brought by different interferences in a cost-effective manner.

## I. INTRODUCTION

Recently attention has been given to the concept of fix-mobile convergence to solve the indoor coverage/capacity problem. User-deployed femtocells, which cover a radius of up to several tens of meters, can be used to provide high-data rate sustained services in the indoor scenario. The use of femtocells brings a multitude of benefits, including enhanced coverage and capacity for indoor applications, better user experiences, and reduced capital and operational costs as a result of delegating indoor services from the macrocells to femtocells [1].

Such deployment of the self-organized femtocells results in a hierarchical structure where femtocells co-exist within the same band and physical location as the well planned macrocell networks. The co-channel interference that the femtocell introduces to the macrocell could potentially compromise the system performance. On the other hand, macro-connected UEs (macro-UEs) can also interfere with femtocells and cause severe degradation in the femtocell receiver performance. In extreme cases a macro-UE in the vicinity of the femtocell could completely jam the femtocell since the macro-UE transmits at high power level to maintain the link margin to the macro base station (BS), which could be hundreds of meters away. The analysis of such interaction between the macro system and the femtocell system has attracted attention from the research community [1].

Claussen *et.al* [2], [3] evaluated the impact of deploying femtocells on existing co-channel macrocells, where their work is based on system level simulations. Chandrasekhar

*et al.* proposed analytic methods in [4], [5] to investigate different uplink interference scenarios in the macrocell and femtocell co-channel deployment environment based on the outage probabilities. However, only in-cell macro interference was considered. Das and Ramaswamy [6] computed the reverse link capacity of femtocells by modeling the interference from surrounding femtocells as the Gaussian random variable, and excluding the interference from the co-channel macrocells. In an extended work [7], Das and Ramaswamy modeled co-channel macrocell interferences as the independent Gaussian random variable, which made reverse link capacity with the consideration of both femtocell and macrocell available.

In this paper, we propose an analytical model to investigate the coverage and capacity of the hierarchical networks through interference analysis. More specifically, we start from a geometric model [8], and formulate the interference for femto-UE to HNB, femto-UE to macro BS and macro-UE to HNB interference scenarios. Without losing the generality, we do not approximate the interference by Gaussian random variable as in [6], [7]. Given the femtocell deployment density, and based on the interference analysis and target SIR defined in the UMTS system [9], we can derive the upper bound of the number of users supported in macrocell and the minimum spreading factor supported in femtocell. Therefore, the capacity of the femtocell can be obtained. Furthermore, using this approach, we are able to study various receiver techniques to improve uplink system performance.

The rest of the paper is organized as follows. In Section II, a generic femtocell model is delineated and assumptions on system topology and network management are stipulated. In Section III, we categorize the interferences between the femtocells and macrocells and evaluate the interference and noise rises caused by them. In Section IV, we present the capacity analysis based on the proposed analytical model. The numerical results on interference investigation are then presented in Section V, together with signal processing techniques to address these interferences. we also present the coverage and capacity results for the femto and macro co-existing network. Section VI concludes the paper.

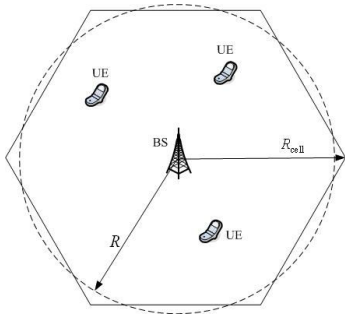


Fig. 1. Macrocell and co-channel femtocell

## II. SYSTEM MODEL

### A. Network Topology

Fig. 1 shows the structure of a hexagon-shaped macrocell, where  $R_{\text{cell}}$  is the radius for the hexagonal cell and  $R$  is the radius of an approximated circle-shaped cell, with the two related by

$$R = \left( \frac{3\sqrt{3}}{2\pi} \right)^{1/2} R_{\text{cell}}. \quad (1)$$

Macrocell BS is installed in the geometrical center of the cell, while macro-UEs are uniformly distributed in the cell. Femtocells are assumed to service a circular region of a radius  $R_f$ , which is typically much smaller than that of  $R$ . The distributions of femtocell HNBs in a macrocell and femto-UEs (UEs attached to HNB) in a femtocell are also assumed to be uniform.

### B. Pathloss Model

Indoor pathloss propagation is drastically different from that for outdoor transmission. Therefore a different pathloss model is applied to femtocells, shown in Table I together with that for the outdoor transmission.

### C. Modeling Assumptions

We make a few assumptions which are summarized as follows.

- AS1 Assume that 10% of the macrocell area is occupied by residences with femtocells, and the ratio of building area to the total block size is 1 : 5.
- AS2 Assume that there are  $M$  femto-UEs serviced by each HNB, and  $N_{mf}$  macro-UEs located inside each femtocell.
- AS3 The loss for electromagnetic signals to go through brick walls is dominated by the shielding loss  $L_s$ , as in Table I.
- AS4 The additional interference introduced by femto-UEs to the macrocell BS is less than  $\eta = 10\%$ .
- AS5 Perfect power management is performed by macrocell BSs and femtocell HNBs, that means, the receive powers of all UEs are the same at the serving base stations.
- AS6 Handover is based on the UE's location (rather than actual receive power), and closed access is employed by HNBs.

From AS1, it can be deduced that the percentage of the net area occupied by femtocells is  $\alpha = 2\%$ . The density of

TABLE I  
SYSTEM PARAMETERS FOR MACRO-FEMTO CO-EXISTING NETWORKS

	Description	Value
$SF_{mue}$	Spread factor (SF) for macro-UEs	128
$SF_{fue}$	SF for femto-UEs	1 - 128
$G_{tx,ue}$	Tx antenna gain of UEs	0 dBi
$L_{tx,ue}$	Tx antenna loss of UEs	0 dB
$G_{rx,BS}$	Rx antenna gain of macrocell BS	10 dBi
$L_{rx,BS}$	Rx antenna loss of macrocell BS	0 dB
$N_{f,BS}$	Noise figure (NF) of macrocell BS	5 dB
$B_{l,BS}$	Body loss (BL) of macro-UEs	2 dB
$SIR_{BS}$	target SIR for macrocell BS	3.2 dB
$G_{rx,HNB}$	Rx antenna gain of HNB	0 dBi
$L_{rx,HNB}$	Rx antenna loss of HNB	0 dB
$N_{f,HNB}$	NF of HNB	7 dB
$B_{l,HNB}$	BL of femto-UEs	4 dB
$P_{t,mue}$	maximum Tx power of macro-UEs	1 W
$P_{t,fue}$	maximum Tx power of femto-UEs	125 mW
$\delta$	reserved power buffer for macro-UE	5 dB
$SIR_{fcb}$	target SIR for HNB	3.2 dB
$R_c$	chip rate	3.84 Mcps
$R_{code}$	channel coding rate	1/2
$M$	number of users per femtocell	2
$N_{mf}$	number of macro-UEs per femtocell	1
$L_s$	external wall shielding loss	10 dB
$R_f$	radius of femtocells	20 m
$R_{min}$	minimum distance btw. HNB and BS	30 m
	outdoor propagation path loss model	$133 + 35 \log_{10}(r)$ dB
	indoor propagation path loss model	$98.5 + 20 \log_{10}(r)$ dB

femtocells, defined as the number of femtocells ( $N_f$ ) in an unit area, is given by

$$\rho_f = \frac{N_f}{A} = \left( \frac{\alpha A}{\pi R_f^2} \right) / A = \frac{\alpha}{\pi R_f^2}. \quad (2)$$

The density of macro-UEs and femto-UEs can be obtained as

$$\rho_{mue} = \frac{K_d}{\pi R^2(1 - \alpha)}, \quad \rho_{fue} = \frac{M}{\pi R_f^2}, \quad (3)$$

where  $K_d$  is the number of UEs in a cell serviced by the macrocell BS. The total number of femtocell users in one macrocell can then be calculated as

$$K_f = M \rho_f \pi R^2 = M \alpha \left( \frac{R}{R_f} \right)^2. \quad (4)$$

## III. INTERFERENCE ANALYSIS

For conventional WCDMA systems, co-channel uplink interferences include the interference from macro-UEs in the same cell as well as those in neighboring cells. However, the issue becomes more complex for the femto and macro co-existing uplink channels where the femto-UE to HNB, femto-UE to macro BS and macro-UE to HNB interferences are present, in addition to the well-studied macro-UE to macro BS interference.

### A. Macro-UE to Macro BS Interference Scenario

1) *Intracell Macro-UE to Macro BS Interference*: In a cellular system with perfect power management, all macro-UEs in the target macrocell are received at the same power

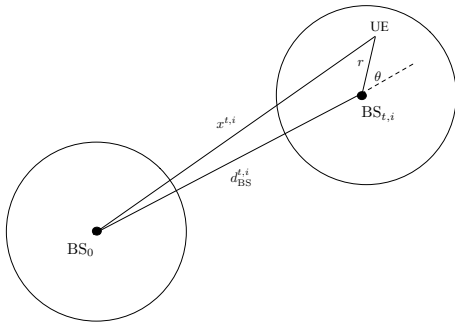


Fig. 2. Geometry of a neighboring-cell UE to the target macrocell  $BS_0$ .

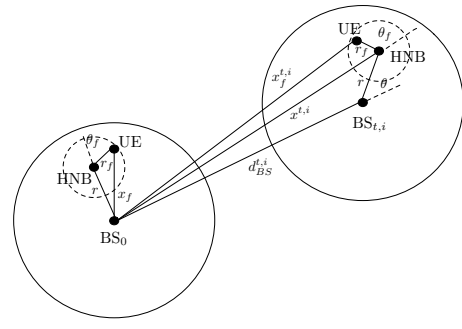


Fig. 3. Geometry of femto-UEs to the target macrocell  $BS_0$ .

$P_{BS}$ . Therefore, the intracell interference to the user of interest is given by

$$I_{mb}^{BS_0} = \sum_{i \neq k, i \in \mathcal{B}_0} P_{BS,i} = (K_d - 1)P_{BS}, \quad (5)$$

where  $\mathcal{B}_0$  denotes the UE set serviced by the base station  $BS_0$ .

2) *Inter-cell Macro-UE to Macro BS Interference*: The intercell macro-UE to Macro BS interference is the sum of those from UEs in neighboring cells. Given the hexagonal cell structure, the cell of interest, i.e., that is serviced by the base station  $BS_0$ , is surrounded by  $T$  tiers of neighboring cells, with the  $t$ -th tier consists of  $6t$  cells. In this paper, we let  $T = 3$  as the interference beyond this range is marginal.

$$I_{mb}^{BS_t} = \sum_{t=1}^T \sum_{i=0}^{6t-1} I_{mb}^{t,i}, \quad (6)$$

where  $I_{mb}^{t,i}$  denotes the uplink interference from the macro-UEs located in  $i$ -th cell of  $t$ -th tier (cell- $(t, i)$ ).

The geometry of an UE in cell- $(t, i)$  to  $BS_0$  is shown in Fig. 2, where  $r$  is the distance between the UE and its serving base station  $BS_{t,i}$ ,  $\theta$  is the azimuth w.r.t. the virtual line linking  $BS_0$  and  $BS_{t,i}$  and  $d_{BS}^{t,i}$  is the distance between the two base stations, given by

$$d_{BS}^{t,i} = |(\sqrt{3}tR_{\text{cell}} + \sqrt{3}(i \bmod t)R_{\text{cell}})e^{j\frac{2\pi}{3}} \times e^{j[\frac{i}{t}]\frac{\pi}{3}} e^{j\frac{\pi}{6}}|. \quad (7)$$

And the distance between the interfering UE and  $BS_0$  can be obtained as

$$x^{t,i}(r, \theta) = \sqrt{r^2 + |d_{BS}^{t,i}|^2 + 2r|d_{BS}^{t,i}|\cos\theta}. \quad (8)$$

The accumulative interference from macro-UEs serviced by  $BS_{t,i}$  is then given by

$$\begin{aligned} I_{mb}^{t,i} &= \mathbf{E} \left[ \iint_{\mathbf{S}_{muc}(t,i)} \rho_{muc} P_{BS} \left( \frac{r}{x^{t,i}(r, \theta)} \right)^{\mu_{BS}} r dr d\theta \right] \\ &= \frac{K_d P_{BS}}{\pi R^2} \int_0^R \int_{-\pi}^{\pi} \left( \frac{r}{x^{t,i}(r, \theta)} \right)^{\mu_{BS}} r dr d\theta, \end{aligned} \quad (9)$$

where  $\mu_{BS} = 3.5$  is the path loss exponent for macrocell radio link in the Hata's model, as given in II-C, and  $\mathbf{S}_{muc}(t, i)$ , whose area is equal to  $(1 - \alpha)\pi R^2$ , is the macrocell coverage

(excluding the area occupied by femtocell) in cell- $(t, i)$ , and can be viewed as a random event due to the randomly distribution of femtocell. The expectation in the above equation is taken over all the possibility of different kinds of femtocell deployment on  $\alpha$  part of  $BS_{t,i}$  area. Substitute equation (9) into (6), we can obtain

$$I_{mb}^{BS_t} = \frac{K_d P_{BS}}{\pi R^2} \sum_{t=1}^T \sum_{i=0}^{6t-1} \int_0^R \int_{-\pi}^{\pi} \left( \frac{r}{x^{t,i}(r, \theta)} \right)^{\mu_{BS}} r dr d\theta. \quad (10)$$

It is observed that the macro-intercell interference in (10) is in terms of  $K_d P_{BS}$ , which is the sum of the receive power of macro-UEs at the serving base station.

### B. Femto-UE to Macro BS Interference Scenario

1) *Intracell Femto-UE to Macro BS Interference*: The geometry of femto-UEs to target base station  $BS_0$  is shown in Fig. 3. The co-channel interference from a femtocell of  $r$  away from  $BS_0$  is given by

$$\begin{aligned} I_{fb}(r) &= \int_{-\pi}^{\pi} \int_0^{R_f} \frac{\rho_{fue} P_f \kappa_f}{L_s \kappa_{BS}} \left( \frac{r_f^{\mu_f}}{x_f^{\mu_{BS}}} \right) r_f dr_f d\theta_f \\ &= \frac{M P_f \kappa_f}{\pi R_f^2 \kappa_{BS} L_s} \int_{-\pi}^{\pi} \int_0^{R_f} \left( \frac{r_f^{\mu_f+1}}{x_f^{\mu_{BS}}} \right) dr_f d\theta_f, \end{aligned} \quad (11)$$

where  $\mu_f = 2$  and  $\kappa_f = 38.5$  are the path loss exponent and constant for indoor radio link,  $\kappa_{BS} = 28$  is the path loss constant for macrocell radio link,  $L_s$  is the shielding loss for wireless go through the femtocell boundary, as given in II-C, and  $x_f = \sqrt{r^2 + r_f^2 + 2rr_f \cos\theta_f}$  is the distance between the femto-UE and  $BS_0$ , in which  $r_f$  and  $\theta_f$  are marked in Fig. 3. The total interference from femto-UEs in the target macrocell is then given by

$$\begin{aligned} I_{fb}^{BS_0} &= \int_{R_{\min}}^R \rho_f I_{fb}(\vec{r}) 2\pi r dr \\ &= \frac{2\kappa_f \rho_f M P_f}{R_f^2 \kappa_{BS} L_s} \int_{R_{\min}}^R \int_{-\pi}^{\pi} \int_0^{R_f} \left( \frac{r_f^{\mu_f+1}}{x_f^{\mu_{BS}}} \right) r dr dr_f d\theta_f, \end{aligned} \quad (12)$$

where  $R_{\min}$  is the minimum distance between femtocells and  $BS_0$ , and introduced to avoid the significant interference from femto-UEs.

2) *Intercell Femto-UE to Macro BS Interference*: The co-channel interference from femto-UEs located in external macrocells is another interfering source that needs to be taken into account in network management. Similar to its counterpart of macrocell UE to macro BS scenario, the intercell femto-UE to macro BS interference is given by

$$I_{fb}^{BS_t} = \sum_{t=1}^T \sum_{i=0}^{6t-1} I_{fb}^{t,i}, \quad (13)$$

where  $I_{fb}^{t,i}$  denotes the interference from femto-UEs in cell- $(t, i)$ . Through some mathematical manipulation, it can be shown that

$$\begin{aligned} I_{fb}^{t,i} &= \int_{-\pi}^{\pi} \int_0^R \rho_f I^{t,i}(r, \theta) r dr d\theta \\ &\approx \frac{2\rho_f \kappa_f M P_f}{(\mu_f + 2) L_s \kappa_{BS}} \int_{-\pi}^{\pi} \int_0^R \left( \frac{R_f^{\mu_f}}{|x^{t,i}(r, \theta)|^{\mu_{BS}}} \right) r dr d\theta. \end{aligned} \quad (14)$$

*Remarks*: Both intracell and intercell femto-UE to macro BS interferences are in terms of  $M P_f$ , which is the total receive power at the femtocell HNB. Regulation on the  $P_f$  is necessary to minimize  $I_{fb}^{BS_t}$  and  $I_{fb}^{BS_0}$  so that the femto-UE to macro BS interferences only result in a marginal loss on the macrocell throughput.

### C. Macro-UE to HNB Interference Scenario

Compared to the effect on macrocells brought by the femto-cells, the macro-UE to HNB interference draws more attention as macro-UEs typically transmit at a power level orders of magnitude higher than femto-UEs. Therefore, significant interference would be generated if there happens to be active macro-UEs at the proximity of the femtocell.

1) *Intracell Macro-UE to HNB Interference*: If an UE enters the coverage of the femtocell while still uses the service of the macrocell base station, it typically generates tremendous interference to the femtocell communication. We refer to this type of macrocell uplink interference to the HNB receiver as the intracell macro-UE to HNB interference. For macro-UEs to maintain a quality link, the transmitted signals need to be sent at a power level much higher than that for an outdoor UE to overcome the shielding loss caused by the external wall of home; otherwise the macro-UE will switch off or back to legacy networks (such as GSM). More specifically, the intracell macro-UE to HNB interference caused by one macro-UE (assumed in AS2) which is  $r_f$  away from femtocell and  $r_{BS}$  away from macrocell BS, is given by

$$I_{mh}^{fcb} = \begin{cases} 0, & \text{if } [P_{BS} \kappa_{BS} (r_{BS})^{\mu_{BS}} L_s] \geq P_{t,mue} \\ P_{BS} \frac{\kappa_{BS} (r_{BS})^{\mu_{BS}} L_s}{\kappa_f (r_f)^{\mu_f}}, & \text{otherwise.} \end{cases} \quad (15)$$

2) *Intercell Macro-UE to HNB Interference*: Intercell macro-UE to HNB interference comes from those macro-UEs staying outside of the femtocells. It consists of interference

from those in the cell serviced by  $BS_0$  as well as those from neighboring cells. The former can be calculated as

$$\begin{aligned} I_{mh}^{BS_0} &= \mathbf{E} \left[ \iint_{S_{mue,0}} \rho_{mue} P_{BS} \left( \frac{r}{x_h} \right)^{\mu_{BS}} r dr d\theta / L_s \right] \\ &= \frac{K_d P_{BS}}{\pi R^2 L_s} \int_0^R \int_{-\pi}^{\pi} \left( \frac{r^{\mu_{BS}+1}}{x_h^{\mu_{BS}}} \right) dr d\theta, \end{aligned} \quad (16)$$

where  $x_h = (r^2 + r_h^2 - 2rr_h \cos \theta_h)^{1/2}$  is the distance between the interfering macro-UE and the femtocell HNB.  $r_h$  is the distance between the HNB and the base station  $BS_0$ , and  $\theta_h$  is the azimuth w.r.t. the virtual line linking  $BS_0$  and HNB.  $S_{mue,0}$ , whose area is equal to  $(1 - \alpha) \pi R^2$ , is the macrocell coverage (excluding the area occupied by femtocell) in  $BS_0$ , and can be viewed as a random event due to the randomly distribution of femtocell. While the latter is given by

$$\begin{aligned} I_{mh}^{BS_t} &= \sum_{t=1}^T \sum_{i=0}^{6t-1} I_{mh}^{t,i} \\ &= \frac{K_d P_{BS}}{\pi R^2 L_s} \sum_{t=1}^T \sum_{i=0}^{6t-1} \int_0^R \int_{-\pi}^{\pi} \left( \frac{r}{x_{mh}^{t,i}} \right)^{\mu_{BS}} r dr d\theta. \end{aligned} \quad (17)$$

where  $x_{mh}^{t,i} = [(d_h^{t,i})^2 + r^2 - 2d_h^{t,i} r \cos \theta_h]^{1/2}$  denotes the distance between the external macro-UE and the femtocell HNB, and  $d_h^{t,i}$  is the distance between the HNB and the base station  $BS_{t,i}$ .

### D. Femto-UE to HNB Interference Scenario

The co-channel femto-UE to HNB interference can be analyzed in a similar way to that we use to evaluate the macrocell interference, as femtocells are densely deployed cellular systems of small size. The only difference is that when we consider the intercell interference there is shielding loss to account for.

1) *Intracell Femto-UE to HNB Interference*: Since perfect power management is assumed for femtocell HNB, according to AS5 in Section II-C, the intracell femto-UE to HNB interference is given by

$$I_{fh}^{fcb} = \sum_{i \neq k, i \in \mathcal{F}_0} P_{f,i} = (M - 1) P_f, \quad (18)$$

where  $\mathcal{F}_0$  denotes the UE set serviced by the femtocell of interest.

2) *Intercell Femto-UE to HNB Interference*: The signal leakage from neighboring femtocells is typically very marginal compared to other interferences for two reasons: 1) The transmit power of femto-UEs is very low due to the limited range of femtocells; 2) Signal leakage becomes much weaker after penetrating through multiple walls to reach the femtocell HNB of interest.

## IV. CAPACITY ANALYSIS

In practical WCDMA systems, the target SIR [9] for macrocell BS receiver,  $SIR_{BS}$ , should be:

$$SIR_{BS} \leq \frac{P_{BS}}{(I_{mb}^{BS_0} + I_{mb}^{BS_t}) \times (1 + \eta) + \sigma^2} \cdot \frac{S F_{mue}}{R_{d,mue}}, \quad (19)$$

where  $\eta$  is the allowed noise rise from femtocell interference, and  $\sigma^2$  is the white noise variance, and  $R_{d,mue}$  is the number of information bits contained in each modulation symbol for macro-UEs. The allowed macro-UE number in the center macrocell can be derived in (20) by substituting (5) and (10) into (19).

Similarly, the target SIR for femtocell HNB receiver,  $SIR_{fcb}$ , can be expressed as

$$SIR_{fcb} \leq \frac{P_f}{I_{fh}^{fcb} + I_{mh}^{fcb} + I_{mh}^{BS_0} + I_{mh}^{BS_t} + \sigma^2} \cdot \frac{SF_{fue}}{R_{d,fue}}, \quad (21)$$

where  $R_{d,fue}$  is the number of information bits contained in each modulation symbol for femto-UEs. Hence, the average minimum spread factor for femto-UE,  $SF_{fue}^{\min}$ , which is used to determine the femtocell capacity, can be calculated based on the background interferences from macrocells, the target SIR for femtocell HNB, and the number of femto-UEs per femtocell, as follows

$$SF_{fue}^{\min} = SIR_{fcb} \cdot R_{d,fue} \cdot \left[ (M-1) + \frac{I_{mh}^{fcb} + I_{mh}^{BS_0} + I_{mh}^{BS_t} + \sigma^2}{P_f} \right]. \quad (22)$$

The femtocell capacity are computed as the sum throughput for corresponding UEs as follows:

$$C_{fcb} = \frac{MR_c R_{code} R_{d,fue}}{SF_{fue}^{\min}}, \quad (23)$$

where  $R_c$  is the chip rate and  $R_{code}$  is the channel coding rate.

## V. NUMERICAL RESULTS

### A. Interference and Capacity Analysis at macro BS receiver

Based on the AS1 in Section II-C, the interfering power from femto-UEs to the macrocell base station  $BS_0$  should be less than a certain threshold, i.e.,

$$I_{fb}^{BS_0} + I_{fb}^{BS_t} \leq 10\% (I_{mb}^{BS_0} + I_{mb}^{BS_t}), \quad (24)$$

from which we can deduce that the allowable average transmit power of a femto-UE is  $P_{fem}^{\max} \approx 12.3$  mW. This is below the maximum transmit power listed in Table I, which indicates the necessity to limit the transmission power of femto-UE to avoid the excessive interference to macro BS. In the sequel, we deem  $P_{fem}^{\max}$  as the *de facto* maximum transmit power of femto-UEs. When the macrocell radius is assumed to be  $R = 1000$  meters, the number of active macro-UEs is  $K_d = 36$  from (20).

### B. Interference Splitting at HNB receiver

Based on the results from the macrocell capacity calculation, we evaluate the co-channel interference at the femtocell HNB. Fig. 4 shows different types of interferences at the femtocell HNB at different locations within the macrocell. The interference is normalized w.r.t.  $MP_f$ , the total receive power at the HNB from intracell femto-UEs. It can be seen that the intracell femto-UE to HNB interference is significant, while

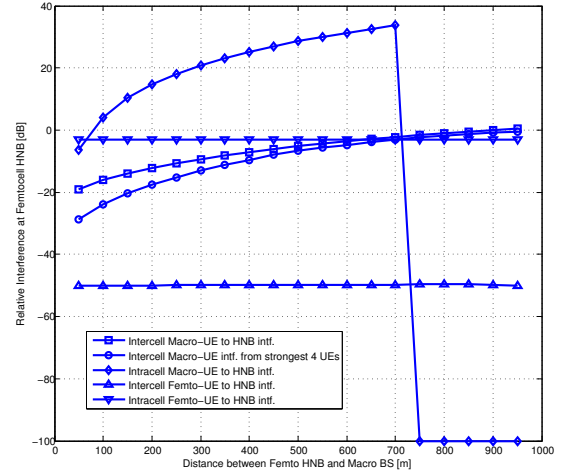


Fig. 4. Co-channel Interference at the HNB for different locations within the macrocell.

the intercell femto-UE to HNB interference is negligible, due to the reasons presented in Section III-D.2. It should be noted that both are constant across the entire macrocell range. On the other hand, the intercell interference from macro-UEs, tends larger as the location of the HNB approaches the border of the macrocell, due to the increasing transmit power of macro-UEs in the outer region.

1) *Intracell Macro-UE to HNB Interference*: It is shown by Fig. 4 that the power of the intracell macro-UE to HNB interference is dominant within a certain range of the macrocell. It is observed that in the region of  $60\text{m} \leq r \leq 700\text{m}$ , intracell macro-UE to HNB interference exceeds that from the intracell femto-UEs. This marks a donut-shaped *dead-zone* where the intracell macro-UE to HNB interference results in disruption to the femtocell communication, and it deserves great attention in femtocell deployment. It should be noticed that the interference plunges for  $r \geq 700\text{m}$  is due to the fact that macro-UEs can no longer connect to macro BS as mentioned in Section III-C.1.

2) *Intercell Macro-UE to HNB Interference*: The solid line with circles in Fig. 4 shows the relative interference from the most significant 4 intercell macro-UEs at the femtocell HNB receiver across the macrocell. By comparing it with the curve with square, it can be concluded that a few macro-UEs (four in Fig. 4) contribute to most of the interference, more than 50% of the total interference from intercell macro-UEs, in region of  $r \geq 450\text{m}$ . Straightforwardly, this result indicates the potential importance and practicability to deal with the strongest interferences from intercell macro-UEs.

### C. Capacity and Coverage

Fig.5 shows the per-user data throughput for femto-UEs at different locations across the macrocell. It should be noticed that in realistic systems the maximum uplink data throughput would be restricted to some maximum value, we do not restrict the data rates here to show the benefits of interference cancellation.

$$K_d \leq \frac{SF_{muc} / [R_{d,muc} SIR_{BS}] - \sigma^2 / P_{BS} + (1 + \eta)}{(1 + \eta) \left[ 1 + \sum_{t=1}^T \sum_{i=0}^{6t-1} \int_0^R \int_{-\pi}^{\pi} \frac{1}{\pi R^2} \left( \frac{r}{x^{t,i}(r,\theta)} \right)^{\mu_{BS}} r dr d\theta \right]} \quad (20)$$

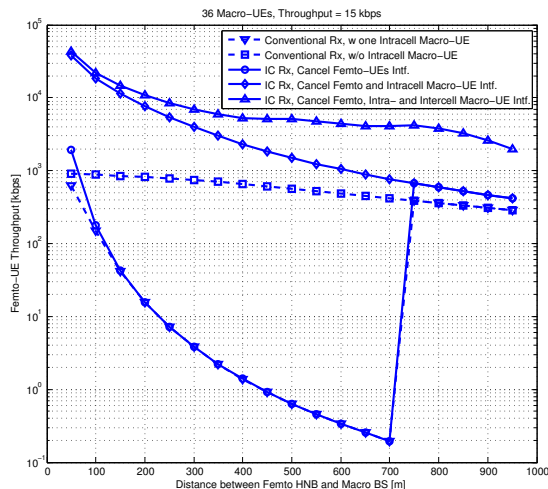


Fig. 5. Femto-UE throughput at different locations within the macrocell.

If there aren't any macro-UEs located inside the femtocell, the throughput of femto-UEs using conventional technology can be above 200 kbps across the macrocell. However, if we assume there is one macro-UE inside each femtocell, the throughput plummets down to a few kilobits per second, indicating a very limited service in this region.

It is well known that the severe uplink throughput impairment due to the macro-UE aggressor could be significantly overcome to a large degree through the pragmatic mechanism of adaptive uplink attenuation [10]. Different from that, we consider a number of advanced receiver schemes with multiuser detection capabilities (called IC Rx for Interference Cancelling Receivers) to overcome this problem in this paper. The solid line with circles in Fig. 5 represents the resultant data rate for an advanced receiver which tackles the intracell femto-UE to HNB interference. It can be seen that for this scheme the improvement in the *dead zone* is marginal, while the throughput is raised to a few hundred of kbps outside of the *dead zone*. The solid line with diamonds is for the advanced receiver canceling both intracell femto-UE to HNB and intracell macro-UE to HNB interference. As a result, there is no noticeable *dead zone*. On the other hand, the achievable throughput degrades rapidly as the femtocell location approaches the macrocell border, due to the increasing intercell macro-UE to HNB interference. The third advanced receiver is then proposed to address most significant intercell macro-UE to HNB interference. The so obtained throughput is shown in Fig. 5 by the solid curve with triangles. The improvement compared to the other advanced receivers become significant as the femtocell stays away from the macrocell base station, with the data throughput at the cell border being increased by an order of magnitude.

## VI. CONCLUSION

In this paper, we proposed an analytical model to study the uplink capacity and coverage of UMTS femtocells co-existing within the macrocells. We started from a hierarchical geometric model and analyzed the macrocell and femtocell interference scenarios. Based on this comprehensive interference analysis, we derived the macrocell and femtocell capacity based on practical target SIR approach. We show through numerical results that the presence of macro-UEs entering femtocell area in the *dead-zone* and macro-UEs outside the femtocell which approach the macrocell border generate significant interference than other interference scenarios. We further show that advanced receivers with the capability to cancel the interference from intracell and intercell macro-UE to HNB interferences would improve the system capacity dramatically.

## ACKNOWLEDGMENT

H. Wang is with the Australian National University and NICTA. M. Zhao and M. C. Reed are with NICTA and the Australian National University. NICTA is funded by the Australian Government as represented by the Department of Broadband, Communications and the Digital Economy and the Australian Research Council through the ICT Centre of Excellence program. Z. Shi was with NICTA and the Australian National University when the work was done and is currently with Alcatel Lucent-Shanghai Bell.

## REFERENCES

- [1] V. Chandrasekhar, J. Andrews, and A. Gatherer, "Femtocell networks: a survey," *IEEE Commun. Mag.*, vol. 46, no. 9, pp. 59–67, Sept. 2008.
- [2] H. Claussen, "Performance of macro- and co-channel femtocells in a hierarchical cell structure," in *Proc. IEEE 18th Int'l Symp. on Personal, Indoor and Mobile Radio Commun. (PIMRC'07)*, Sept. 2007, pp. 1–5.
- [3] —, "Co-channel operation of macro- and femtocells in a hierarchical cell structure," *Int'l. J. Wireless Inform. Networks*, vol. 15, no. 3-4, pp. 137–147, 2008.
- [4] V. Chandrasekhar and J. Andrews, "Uplink capacity and interference avoidance for two-tier cellular networks," in *Proc. IEEE Global Commun. Conf. (GLOBECOM'07)*, Nov. 2007, pp. 3322–3326.
- [5] —, "Uplink capacity and interference avoidance for two-tier femtocell networks," *IEEE Trans. Wireless Commun.*, vol. 8, no. 7, pp. 3498–3509, July 2009.
- [6] D. Das and V. Ramaswamy, "On the reverse link capacity of a CDMA network of femto-cells," in *Proc. IEEE 31st Sarnoff Symp. (SARNOFF'08)*, Apr. 2008, pp. 1–5.
- [7] V. Ramaswamy and D. Das, "Multi-carrier macrocell femtocell deployment—a reverse link capacity analysis," in *Proc. IEEE 70th Vehic. Tech. Conf. (VTC'09-Fall)*, Sept. 2009, pp. 1–6.
- [8] Z. Dawy, S. Davidovic, and I. Oikonomidis, "Coverage and capacity enhancement of cdma cellular systems via multihop transmission," in *Proc. IEEE Global Commun. Conf. (GLOBECOM'03)*, vol. 2, Dec. 2003, pp. 1147–1151.
- [9] *Physical Layer Procedures (FDD)*, 3GPP Std. TS25.214 Rel-7, 2008.
- [10] M. Yavuz, F. Meshkati, S. Nanda, A. Pokhariyal, N. Johnson, B. Raghathan, and A. Richardson, "Interference management and performance analysis of UMTS/HSPA+ femtocells," *IEEE Commun. Mag.*, vol. 47, no. 9, pp. 102–109, Sept. 2009.